
Masters Theses

Student Theses and Dissertations

1966

Absolute soft x-ray dosimetry for radiation chemistry studies

Howard Sajon Joyner

Follow this and additional works at: https://scholarsmine.mst.edu/masters_theses



Part of the [Physics Commons](#)

Department:

Recommended Citation

Joyner, Howard Sajon, "Absolute soft x-ray dosimetry for radiation chemistry studies" (1966). *Masters Theses*. 2943.

https://scholarsmine.mst.edu/masters_theses/2943

This thesis is brought to you by Scholars' Mine, a service of the Missouri S&T Library and Learning Resources. This work is protected by U. S. Copyright Law. Unauthorized use including reproduction for redistribution requires the permission of the copyright holder. For more information, please contact scholarsmine@mst.edu.

ABSOLUTE SOFT X-RAY DOSIMETRY FOR RADIATION
CHEMISTRY STUDIES

by

H. SAJON JOYNER - 1934

A

THESIS

submitted to the faculty of

THE UNIVERSITY OF MISSOURI AT ROLLA

in partial fulfillment of the requirements for the

Degree of

MASTER OF SCIENCE IN PHYSICS

Rolla, Missouri

1966

123720

T 1967
e.1

59 P.

Olto H. Hill (advisor) J. R. Faucett

J. R. Faucett

D. R. Edwards

ABSTRACT

A homogeneous, variable plate separation ion chamber consisting of a polyethylene body and employing flowing ethylene as the cavity gas has been designed and tested for the specification soft x-ray (<75kV) energy deposition in typical hydrocarbons. The variable plate separation feature provided primary data on the differential specific ionization originating within the cavity gas occupying the effective collector volume which is independent of inherent chamber inhomogeneities associated with the electrically conducting films comprising the chamber electrodes. These data demonstrated that charged particle equilibrium is established within the first few ten thousandths of an inch in typical solid hydrocarbons irradiated with this class of sources. Comparison of this type of chamber with a fixed plate separation, static cavity gas mode of operation showed that the latter may predict dose rates with inherent errors exceeding 100%. With the quality of electronic readout accessories presently available, the variable plate separation chamber yielded dose rate data exhibiting a probable error of 3.8 percent (plus the unknown uncertainty in the literature data on the energy required to form an ion pair), and an ultimate limiting error of less than 2 percent appears feasible.

ACKNOWLEDGEMENT

I wish to thank Dr. Otto H. Hill for his suggestion of the problem and his many helpful discussions about the experiment. I also wish to thank the Graduate Center for Materials Research of the Space Science Research Center of the University of Missouri at Rolla for financial support.

January, 1967

H.S.J.

TABLE OF CONTENTS

	Page
LIST OF FIGURES	vi
I. INTRODUCTION	1
A. Radiation Chemistry	1
B. Methods of Specification of Energy Deposition	3
C. Soft X-Ray Energy Deposition	3
II. Theory	6
A. Ion Chamber	6
B. Absorbed Dose	7
C. Determination of W	7
D. Backscattering	8
E. Chamber Inhomogeneities	9
F. Collection Efficiency	9
G. Polarity Effect	11
III. EXPERIMENTAL PROCEDURE	12
A. Radiation Source	12
B. Description of Dosimeter	12
C. Deductions of X-Radiation Energy Deposition	15
1. Analysis of Factors Contributing to the Amount of Cavity Gas Associated with the Ionization	16
a. Analysis of Effective Volume	16
b. Analysis of the Pressure and Temperature of the Cavity Gas	25
c. Compressibility Factor	26
2. Ionization Current Considerations	26
a. Ionization Current Corrections	27
1. Divergence Correction	28
2. Inhomogeneity Correction	28
b. Flowing Gas vs. Static Gas	44
c. Collection Efficiency	47
d. Dose Rate Profile as a Function of Depth	47
IV. RESULTS AND CONCLUSION	53
A. Differential Ionization	53
B. Dose Rate Resolution	54

APPENDIX 56

BIBLIOGRAPHY 58

VITA 59

LIST OF FIGURES

	Page
1. Cross-section of Dosimeter.	14
2. Equipotential Lines of Ion Chamber.	19
3. Voltage Between Collector and Guard Ring vs. Plate Separation	21
4. Voltage Between Window and Collector vs. Plate Separation.	24
5. Sketch of Thermocouple Sensor for Cavity Gas	26
6. $\log_{10} I \times 10^8$ vs. $\log_{10} (d+L/2)$	30
7. Table of Divergence Correction, Alpha	32
8. Integrated Specific Ionization vs. Plate Separation for Aquadeg Window	35
9. Differential Specific Ionization vs. Plate Separation for Aquadag Window	37
10. Integrated Specific Ionization vs. Plate Separation for Beryllium Window	39
11. Differential Specific Ionization vs. Plate Separation for Beryllium Window	41
12. Comparison of Both Integrated and Differential Specific Ionization for Beryllium Window.	43
13. Ionization Current vs. Time After Termination of Cavity Gas Flow.	46
14. Plateau Voltage	49
15. Dose Rate vs. Depth	52

I. INTRODUCTION

A. Radiation Chemistry

Fundamental radiation chemistry studies designed for the purpose of deducing the mechanisms by which material systems react to a radiation environment generally employ experimental techniques in which the integral of the reaction processes are evaluated after exposure to various radiation doses. On the basis of the concentration and types of terminal products obtained from post-irradiation analysis, a series of possible mechanisms are deduced which yield these observed products. In addition to the problems of specifying precise energy deposition, such techniques suffer from several disadvantages among which are (1) loss of environmental and temperature integrity during post-irradiation analytical procedures, (2) lack of resolution in the specification of the rates at which reactions proceed since only the integral is evaluated and (3) the frequent necessity of employing a number of separate samples of the same material with the consequent loss of resolution resulting from sample variations.

If these procedures are to be improved, it is necessary that experimental techniques be sought which provide data on the rates at which these reactions proceed and which incorporate minimum compromise of the environmental and temperature integrity of the sample system. Such an improved technique must be based upon radiation sources

that may be integrally mated to the analytical equipment to be employed.

Relatively low energy (< 75 kv) x-rays represent one class of sources which are readily adaptable to these techniques. They offer several advantages among which are (1) ease of shielding, (2) variable dose rates extending to relatively high intensities (up to 10^{16} ev g^{-1} sec^{-1}), (3) ease of mating to analytical equipment, and (4) satisfaction of conditions of charged particle equilibrium*. The primary difficulty associated with the precision specification of x-ray energy deposition in material systems lies in the fact that the x-rays impinging on the sample have a broad spectrum and are not monochromatic. This difficulty has been responsible for their limited service to date.

*To be in charged particle equilibrium at a point, the International Commission on Radiological Units and Measurements (1) has set forth the following criteria:

Charged particle equilibrium would exist at a point within a medium under irradiation if (a) the intensity and energy spectrum of the primary radiation were constant throughout a region extending in all directions from the point, to a distance at least as great as the maximum range of the secondary charged particles generated by the primary radiation, and (b) the energy absorption coefficient for the primary radiation and the stopping power for the secondary charged particles were constant in the medium throughout the same region as in (a).

B. Methods of Specification of Energy Deposition

Specification with any precision of the energy deposited in the material system has certain inherent difficulties in the dosimetry techniques. The determination of absorbed dose which can be counted on as a reliable standard for comparison between various laboratories falls into three main categories. These are, namely, calorimetric, chemical, and ionization methods. Calorimetric systems operate by absorbing energy from the radiation field and retaining this energy until it is degraded to thermal energy and then evaluates the rise in temperature of the system. The loss of absorbed radiation energy to forms other than heat is a fundamental difficulty in calorimetric measurements; also relatively intense radiation fields must be used with this method. Wet chemistry dosimetry is based on the principle that certain quantitative oxidation and reduction reactions take place upon irradiation which may be related to the absorbed dose. Ultimately the chemical method rests upon either ionization or calorimetric calibration. The ionization method employs the fact that there exists a relation between the ionization produced in a gas filled cavity and the energy imparted in the irradiated material. Other methods include photographic, solid state, and scintillation dosimetry.

C. Soft X-Ray Energy Deposition

In theory there are several methods available for

the specification of energy deposition in materials by soft x-rays. One such method would be to employ information on the absolute spectral energy distribution incident upon the sample and data on the sample x-ray absorption coefficients to deduce the energy deposition in the sample. However, data on the absolute x-ray spectra from conventional x-ray tubes is extremely limited and lacks the necessary precision for radiation chemistry purposes. Aitken and Dixon (2) and Wang, Raridon, and Tidwell (3) give relative spectra from conventional x-ray tubes. The variations in the different relative spectra reported by these authors are such as to make the use of these data questionable for precise radiation chemistry studies. Ehrlich (4) and Epp and Weiss (5) on the other hand give absolute spectral distributions. However, Ehrlich reported an accuracy of ± 30 percent while Epp and Weiss reported a ripple on the x-ray tube voltage and employed a tube with a 15° target angle while commercial tubes use 22° . Since the spectrum is affected by the target angle, the results will be different under other operating conditions.

Another method which offers the possibility of more precision consists of the construction of a homogeneous ion chamber with a body of sample material and a cavity gas having the same composition. There exists a large family of hydrocarbons of the general form $(CH_2)_n$ for

which the construction of such ion chambers is feasible. The design, construction, and employment of one such possible chamber is the subject of the present thesis. A homogeneous, variable plate separation ion chamber made of polyethylene with ethylene as the cavity gas was designed to specify the absolute rates at which energy is deposited by soft x-radiation sources in these typical hydrocarbons.

II. THEORY

A. Ion Chamber

An ionization chamber consists essentially of a gas filled cavity containing electrodes to which a voltage may be applied to collect the ions which are formed in the cavity gas as a result of interaction with a radiation field. There are numerous versions of the geometry, electrode structure, and chamber composition which have been employed for radiation monitoring. There are, however, several operating characteristics which all of these chambers have in common. They are all concerned with measurements of the ionization produced in the cavity gas and the use of this information to deduce the energy deposited in some material system.

When the radiation interacts with the cavity gas, it produces positively charged ions and electrons. Because of the mutual attraction of oppositely charged particles, there is always a tendency for ions to recombine and form neutral atoms. These ions that recombine do not contribute to the externally measured ion current. Thus with low collecting voltages there is a substantial amount of recombination, and many of the ions are lost before they can contribute to the ion current. The fraction lost decreases as the accelerating voltage increases, and eventually all the ions are collected, and there is no further increase in current. This condition is known as

saturation, and the maximum current is called the saturation current. If the voltage is further increased, finally there is a point where the electrons have enough kinetic energy to ionize the gas and the resulting ionization current is no longer representative of the amount of radiation interacting with the cavity gas.

In these experiments the gas used to infer the dissipated energy was employed in a homogeneous ion chamber. The term homogeneous is used to define that system in which the chamber body and the cavity gas have the same chemical composition.

B. Absorbed Dose

If D is the absorbed dose, in ergs, imparted per gram of the material and J_m is the number of ion pairs produced per gram of the gas, then

$$D = J_m W \quad (1)$$

where W is the average energy in ergs given up by the ionizing particles during interaction with the cavity gas for each ion pair which is formed. There are a number of subtleties associated with the specification and meaning of J_m . The most important thing is knowing that when referring to J_m , it is associated only with that part of the sample under the influence of radiation.

C. Determination of W

The average energy W expended in a gas per ion pair

formed is the quotient of E by N_w , where N_w is the average number of ion pairs formed when a charged particle of initial energy E is completely stopped by the gas, $W=E/N_w$. The value of W is determined by an absolute measurement of the charged particle energy loss in the gas and of the resulting ionization. W is usually found by the measurement of the ionization produced by α -particles, γ -rays, or β -rays of known energy. The ionization chamber is sufficiently large that the ionizing particles are totally absorbed. For example, the total ionization produced per second in air by the α -particles from RaC in equilibrium with one gram of radium has been accurately measured. Since both the energy of the RaC α -particles and the number emitted per second is accurately known, W may be evaluated. Whyte (6) pointed out that W is virtually independent of the energy of the particles from high energies down to at least six kilovolts. The relative values of W for different gases for any given source of radiation are generally more accurate than the absolute values which have systematic differences between laboratories. To obtain a weighted mean value of W for the different gases, a mean value for air or a noble gas is used to normalize the data between the laboratories.

D. Backscattering

Backscattering from the back wall of the cavity generated by photoelectrons can also contribute to the

energy deposition in the system. Ogier and Ellis (7) pointed out that the effect of backscattering due to photoelectric absorption is small and indicates the photoelectric quantum yields are usually less than three percent for the photon energies used here.

E. Chamber Inhomogeneities

Inherent inhomogeneities present in typical ion chambers are due to the thinness of the windows allowing for the possibility of electrons produced outside of the chamber to enter and the necessity of conducting films of different chemical composition. In a typical fixed plate ion chamber the inherent chamber inhomogeneities can be corrected by changing the pressure or density of the cavity gas and examining the changes in the induced ionization. However, with thin flexible windows the necessary wide ranges of pressure variations are not feasible. Alternatively, one can increase the amount of cavity gas by using variable plate separation homogeneous ion chambers, which is the method adopted here.

F. Collection Efficiency

An important consideration of the ionization method is the collection efficiency, which is a measure of the degree of saturation. Boag and Wilson (8) have formulated

the collection efficiency in terms of a dimensionless product of the geometric and electrical variables associated with a particular ion chamber. The collection efficiency, f , is shown to be

$$f = \frac{2}{1 + [1 + (2/3) \xi^2]^{1/2}} \quad (2)$$

where

$$\xi = \frac{m d^2 q^{1/2}}{V} \quad (3)$$

and d is the plate separation, q is the charge density per second, V is the collecting voltage, and m is a constant characteristic of the gas, given by,

$$m = [(\alpha/e) k_1 k_2]^{1/2}. \quad (4)$$

α is the recombination coefficient in $\text{cm}^3 \text{sec}^{-1}$, e is the electron charge, and k_1 and k_2 are the positive and negative ion mobilities respectively. According to Erickson (9,10), α/e varies as the inverse of the 7/3 power of the absolute temperature. With $\alpha/e = 3200$ for air (a close approximation for ethylene) at atmospheric pressure and 0°C , a value of $\alpha/e = 2650$ for 23°C was found. Using the same mobility as the electron for the freshly formed positive ion, $k=2.1$, m was found to be $24.5 (\text{esu sec})^{1/2} \text{cm}^{-3/2}$.

Now since $i = f q d$, where i is the ionization current per square centimeter of plate area, and upon introducing a new parameter η , where $6\eta = f\xi^2$, then

$$f = \frac{2}{1 + (1 + 4\eta/f)^{1/2}} \quad (5)$$

This reduces to $f=1/1+\eta$, for large values of $f \rightarrow 1$, where η is dependent upon i and not q . The form for η is $\eta = m^2 i d^3 / 6V^2$.

G. Polarity Effect

Boag (11) has shown that if the ion chamber is operating below complete saturation, then a change in ionization current will be noted when the polarity of the parallel plates is reversed. This effect would be due to an assymetry in the gas of the chamber. The only assymetry encountered in this case is the difference between the mobilities of the positive ions and electrons in the gas.

III. EXPERIMENTAL PROCEDURE

A. Radiation Source

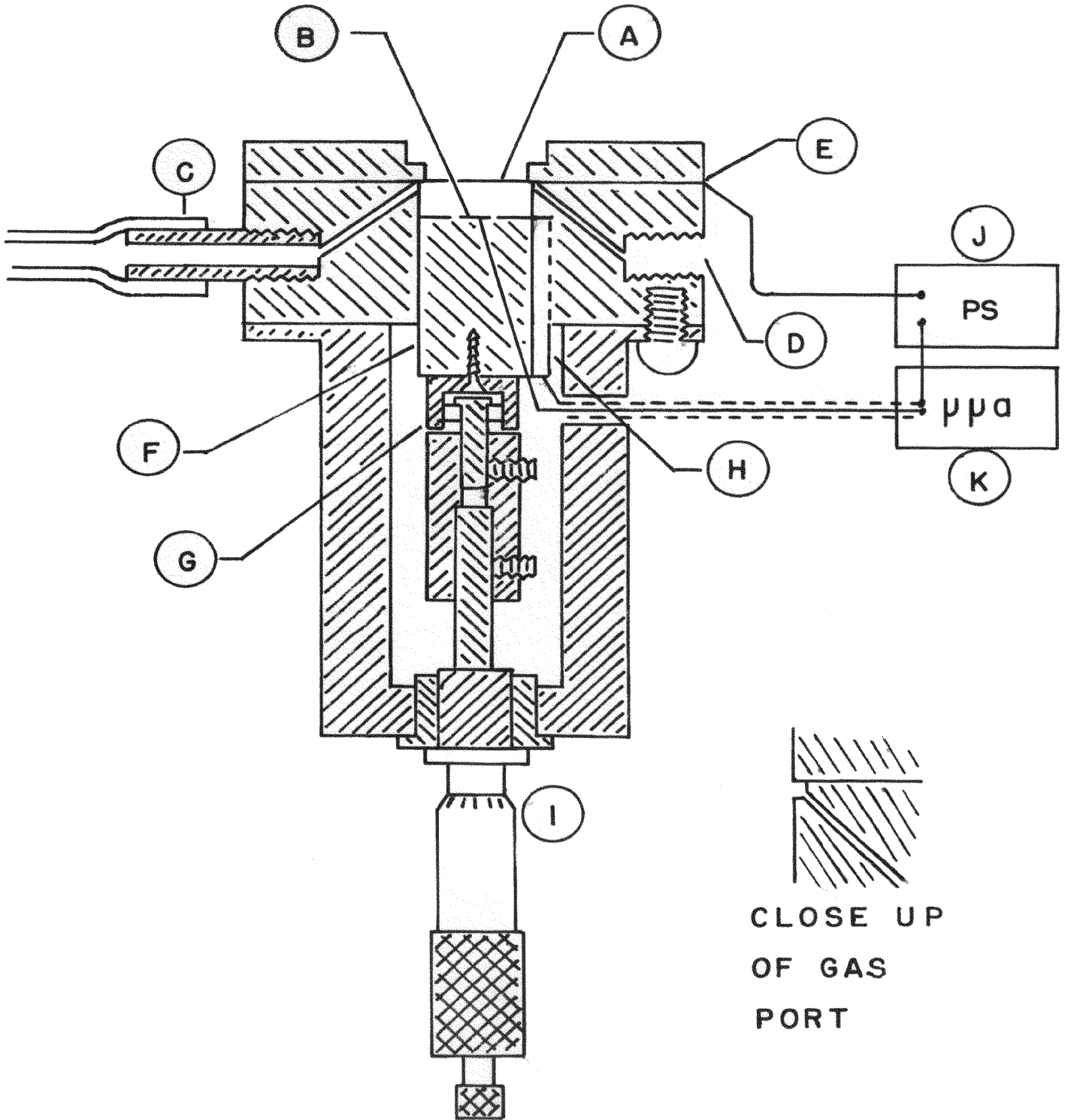
The x-rays for this study were produced by a power supply of a constant voltage type, Model BAL-75-50-UM manufactured by Universal Voltronics Inc. to meet the requirements specified by this laboratory. It possesses a current regulation of 0.1 percent and a voltage regulation of 0.1 percent with a ripple of less than 0.1 percent rms. The power supply is capable of producing 75 kilovolts at a current of 50 milliamperes. The x-ray tube used in these experiments was a G.E. type EA-75 with a maximum operating characteristic of 75 kilovolts constant potential at 37.5 milliamperes.

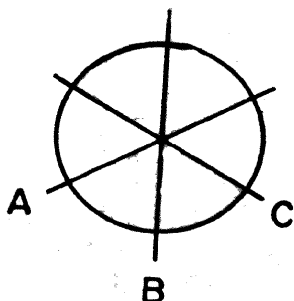
B. Description of Dosimeter

As indicated earlier, a homogeneous ion chamber with variable plate separation and utilizing a polyethylene chamber body and ethylene as the cavity gas was used to determine the rate of energy deposition in solid hydrocarbons by soft x-ray sources. Figure 1 shows a cross-sectional view of the chamber employed in these studies. The cavity volume is cylindrical in geometry, measures 1.50 inches inside diameter, and has a coaxially inscribed circular collector area with a diameter measured to be 0.374 ± 0.001 inches with a traveling microscope. The following are the data for the diameter measurements:

Figure 1

Cross-Sectional View of Dosimeter. A. Front Window, B. Collector, C. Gas Inlet Port, D. Gas Outlet Port, E. Electrical Connection to Front Window, F. Sliding Barrel, G. Ball Bearing Coupler, H. Anti-Rotation Fin, I. Micrometer Barrel, J. Power Supply, K. Picoammeter.





dia.	trial	measurement
A	1	0.9496 cm.
	2	0.9542 cm.
B	1	0.9501 cm.
	2	0.9503 cm.
C	1	0.9529 cm.
	2	0.9500 cm.

The cavity made used of research grade ethylene gas in its cylindrical geometry, and was maintained at atmospheric pressure while flowing continually through the chamber at moderate rates extending from 150 to 180 cc min⁻¹.

C. Deductions of X-Radiation Energy Deposition

The time rate of change of energy deposition per unit mass of gas is given by

$$\frac{dD}{dt} = \frac{I}{e} \frac{W}{nM} \quad (6)$$

where I is the effective ionization current associated with the particular sample geometry, e is the electron charge, W is the energy required to produce an ion pair in the particular gas, n is the number of moles of gas occupying the effective collector volume, and M is the molecular weight of the gas. The specification of the experimental data to be associated with each of the parameters in the above equation requires careful consideration of the factors which alter the values in the experimental geometry employed.

1. Analysis of Factors Contributing to the Amount of Cavity Gas Associated with the Ionization

In computing the value of n in the above equation, the real gas equation was used,

$$\Omega_0 = \frac{PV}{nRT} \quad \text{or} \quad n = \frac{PV}{\Omega_0 RT}, \quad (7)$$

where n is the number of moles of gas occupying the effective collector volume, P is the pressure, V is the volume, T is the temperature, and Ω_0 is the compressibility factor of the gas.

a. Analysis of Effective Volume

To analyze the effective collector volume of a plane parallel plate ion chamber requires a knowledge of the electrical potential gradient existing between the plates. If these field lines are not parallel to the axis of the chamber, then the distortion must be taken into account in a specification of effective collector volume.

One may, for convenience, consider the dosimeter electrically as a capacitor of two parallel circular coaxial conducting discs with its resulting electric field. Nicholson (12) attempted a mathematical description of the potential in terms of spheroidal harmonics, however, Love (13) pointed out the errors in Nicholson's paper and offered a solution to the problem involving a Fredholm integral.

The dosimeter employed here has a volume described by a cylinder with a diameter equal to that of the collector and a length determined by the plate separation. Since the front window is larger than the collector, the dosimeter may be considered to have discs of unequal diameters in the capacitor analogy. This fact coupled with that of Love considering only equal discs in his extension of Nicholson's paper, led to an empirical examination of the problem which is treated in detail in the Appendix. A plot of the resulting equipotential lines shown in Figure 2 showed that in the central region of interest, the lines are parallel. Therefore, the electric field, $E = -\text{grad}(\phi)$, did not bulge out and was parallel to the axis of the dosimeter in this region, assuming that no potential difference exists between the guard ring and the collector.

If a potential difference does exist between the collector and guard ring, Boag (14) has theoretically related this potential to the effective volume in a parallel plate chamber with the plate separation incorporated as a parameter. To examine the extent of this distortion in our chamber, the collector to guard ring voltage was measured during irradiation in the absence of an applied electric field. Figure 3 shows that for a critical case (ie. close plate separation and 70kV x-rays) the voltage differential, $(\Delta\phi)$, between the guard ring

Figure 2

Plot of Equipotential Lines
of Ion Chamber

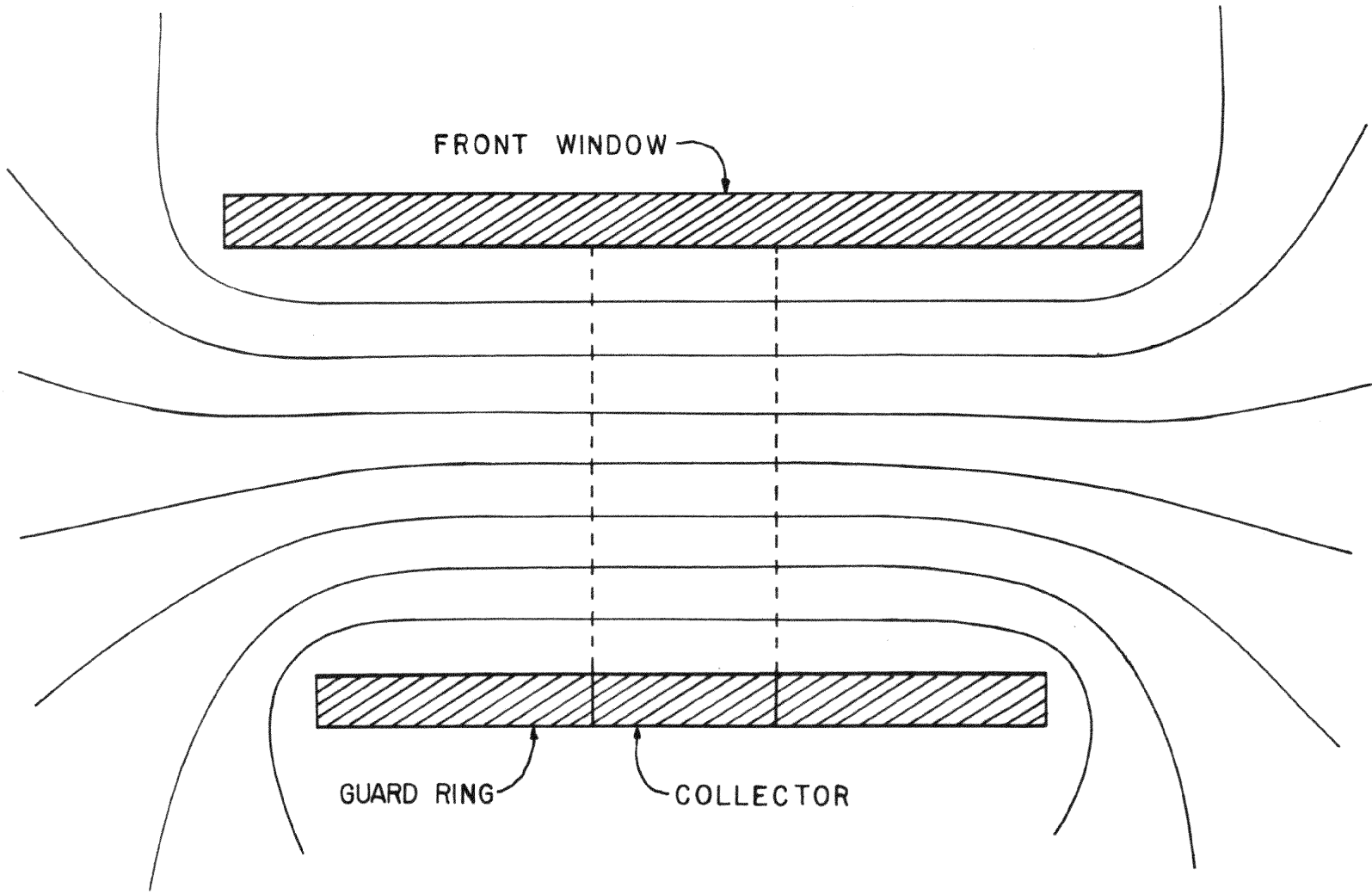
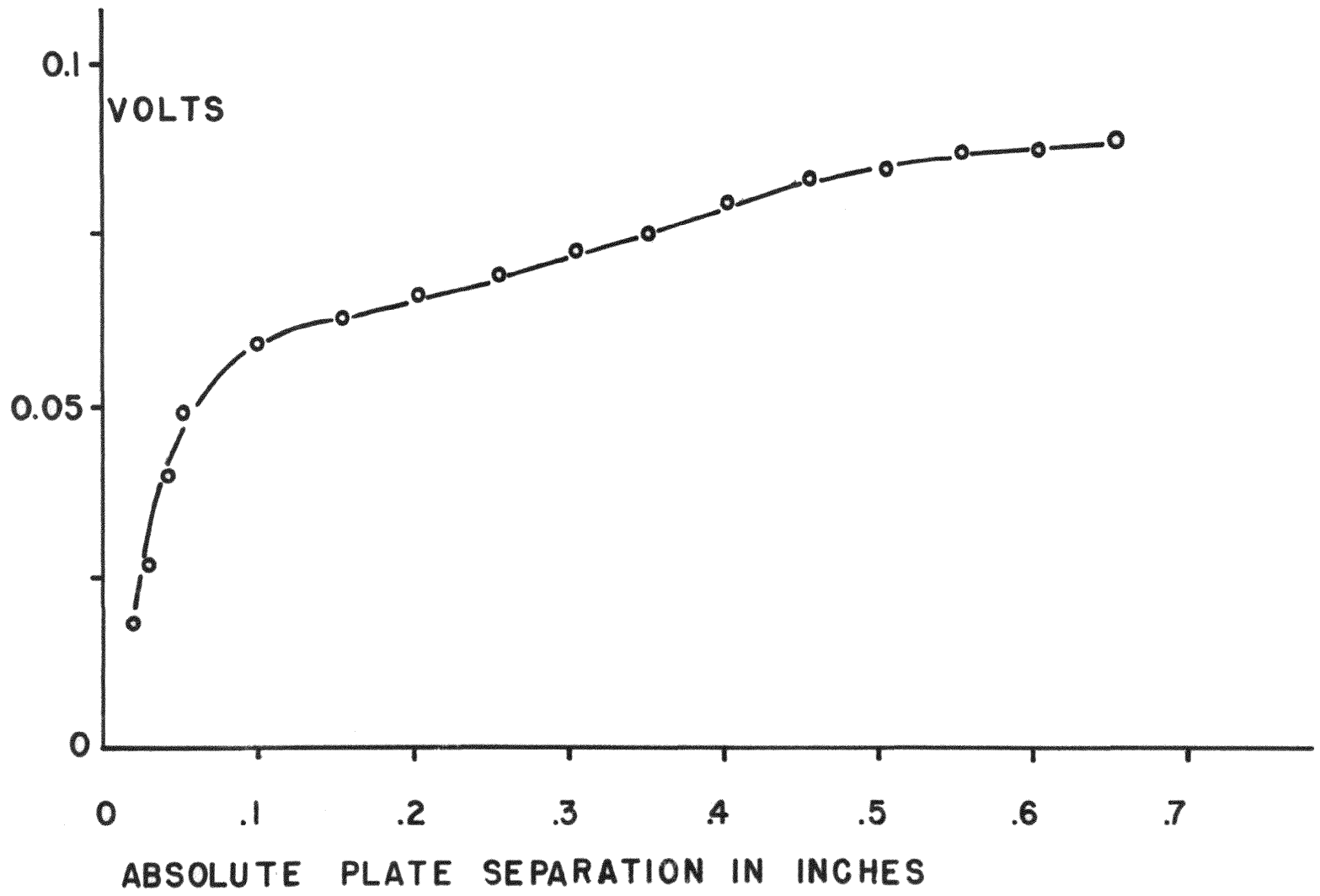


Figure 3

Potential Difference Between the
Collector and Guard Ring vs. Plate
Separation in the Absence of an
Applied Potential. X-ray: 70 kV
at 15 ma. Flow=180 cm³ per minute.

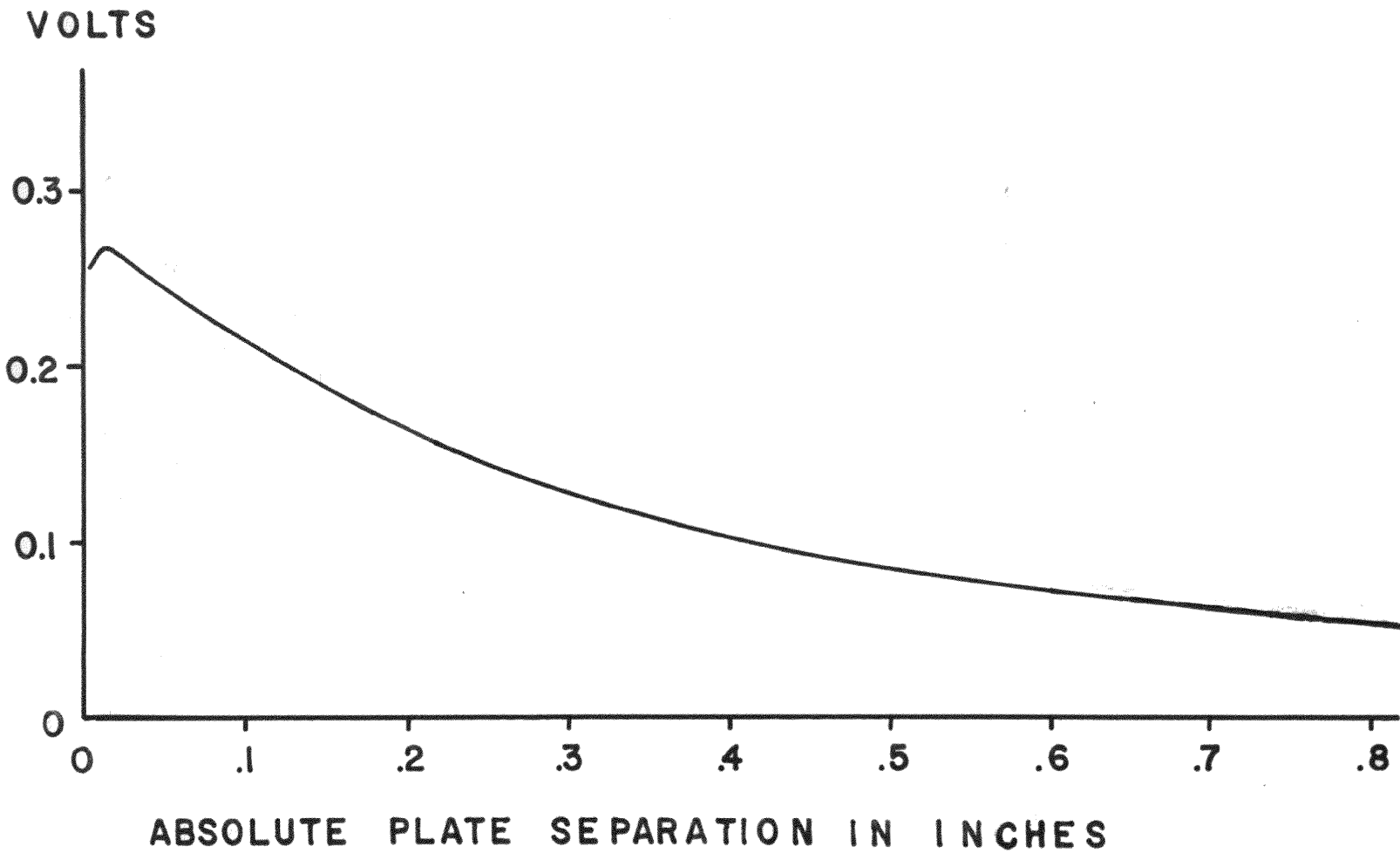


and collector was 0.06 volts at a plate separation of 0.100 inches. At this separation the applied voltage, ϕ , was 200 volts and of the same polarity, which gives a ratio of $(\Delta\phi/\phi)$ equal to 3×10^{-4} . According to Boag's analysis this gives a volume correction of 0.10 percent increase. At a plate separation of 0.500 inches $\frac{\Delta\phi}{\phi}$ is 3.3×10^{-5} , and a resulting volume correction of 0.03 percent was calculated. If the polarity was reversed, there would be a corresponding decrease in volume. However, the actual experiments did not show a detectable ionization current change upon reversal of the electric field.

Along with the radiation field there exists a Compton current due to the generation of free electrons by the radiation within the medium transversed. Hence, the voltage between the collector and front window was measured in the absence of an applied potential to determine if a correction was needed for the voltage required for saturation conditions. Figure 4 shows that the voltage that did appear was a very small percent of the plate voltage and could be attributed to the Compton effect. For example, at a 20 mil separation the plate voltage was 50 volts while the voltage generated in the absence of the applied field was 0.26 volts, hence, no correction was needed. Also as the plate separation increased, the applied voltage increased greatly while the generated voltage decreased.

Figure 4

Potential Difference Between
Window and Collector, Generated
by 70 kV X-rays at 15 ma. in the
Absence of an Applied Field.



At this point a check was made to be sure that the only path for conduction of electric current was through the ionized particles of the gas. Current measurements were made in the absence of a radiation field and no detectable current above background noise of 10^{-12} amperes was observed.

b. Analysis of the Pressure and Temperature of the Cavity Gas.

As can be seen from equation (7), the amount of pressure and temperature can affect the concentration of cavity gas.

Pressure measurements were made on the cavity gas with a Model 121-1 Trans-Sonic Equibar pressure meter with a sensitivity of 0.0002 torr per scale division and reproducibility of 0.1 percent full scale. One leg of the differential pressure analyzer was connected to the ionization chamber by a tube attached to a flat plate which replaced the front window, and the other leg was left at atmospheric pressure. Flow rates from 10 to 180 cubic centimeters per minute caused the pressure inside the cavity to vary from 0.05 to 0.45 torr above atmospheric pressure, respectively.

The temperature measurements were made with a Leeds & Northrup Model 8690 potentiometer having a sensitivity of 0.02 mv per scale division (readable to $\frac{1}{4}$ division or 0.005 mv) connected to 40 gauge Chromel-Alumel thermocou-

ples having a Seebeck coefficient of 0.041mv per °C. The measurements were made in the gas lines at both the entrance and exit port, being careful to isolate the junction from the walls of the tubes as shown in Figure 5.

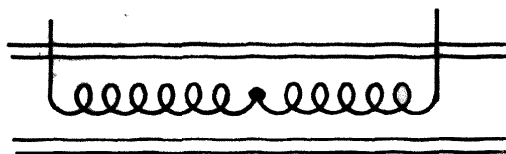


Figure 5

The thermocouple wire was wound in a 1/16 inch diameter coil of approximately ten turns. Fluctuations of less than 0.1°C from room temperature were observed.

c. Compressibility Factor.

The compressibility factor for ethylene was checked and found to be 0.998 using the relationships described by Su (15). As a result no correction to the ideal gas law was employed.

2. Ionization Current Considerations

Current measurements were made with a Keithley Model 417 picoammeter with an accuracy of ± 2 percent of full scale. It is, of course, possible to calibrate the picoammeter to a standard traceable to the National Bureau of Standards which will give a greater accuracy. The output was fed to a Mosely Model 7100A strip chart recorder with an accuracy of 0.2 percent of full scale, and a linearity of 0.1 percent full scale. The factors

influencing the interpretation to be applied to the measurement of the current are discussed in subsequent paragraphs.

a. Ionization Current Corrections

The x-rays emanate from a 5x5mm spot on the x-ray target, and in view of the 3.0 inch target to window distance, they essentially represent a point source. This suggests the possibility that x-ray beam divergence must be considered in the interpretation of ion chamber data. The ion chamber may be conceived as measuring the average rate of ionization on the axis at the midpoint between the plates. As the plate separation increases, the midpoint moves further away from the source. Hence, it appears as though the ion chamber was moving away from the x-ray source. The comparison of ionization currents at different plate separations requires that they be referenced to a common distance from the target. For convenience, the front window of the dosimeter was chosen, since it remains stationary. To normalize the measured ionization current to the front window, a correction factor, α , is defined. Another correction, β , is defined to account for the possible contributions of chamber inhomogeneities to the monitored ionization currents.

The effective ionization current, I , is therefore defined by the product $\alpha\beta i$, where i is the actual ionization

current measured by the picoammeter.

1. Divergence Correction

In order to correct for beam divergence, it was found experimentally that the product of the ionization current and the square of the distance between the x-ray target and the center of the ion chamber was essentially constant for a fixed operating condition of the x-ray source and fixed plate separation of the chamber as shown in Figure 6. Hence, to normalize the measured ionization currents with respect to window position, a divergence correction factor was employed which was defined by,

$$\alpha = \frac{(d + \frac{1}{2}L)^2}{d^2} \quad (8)$$

where d is the distance from the x-ray target to the front face of the ion chamber window, and L is the ion chamber plate separation. A table of α is given in Figure 7 with both 2.00 and 1.98 used as exponents in equation (8). Using 1.98 for the exponent in the alpha correction term gives a small difference in the absolute value of correction to the ionization current over that of 2.00, however, difference data is altered by about one-tenth percent.

2. Inhomogeneity Correction

In a truly homogeneous ion chamber, the ratio of ionization current to chamber volume should be a constant value independent of chamber volume, but if electronic

Figure 6

Log $i \times 10^8$ vs. Log $(d+L/2)$
X-Ray: 70 kV @ 15 ma.

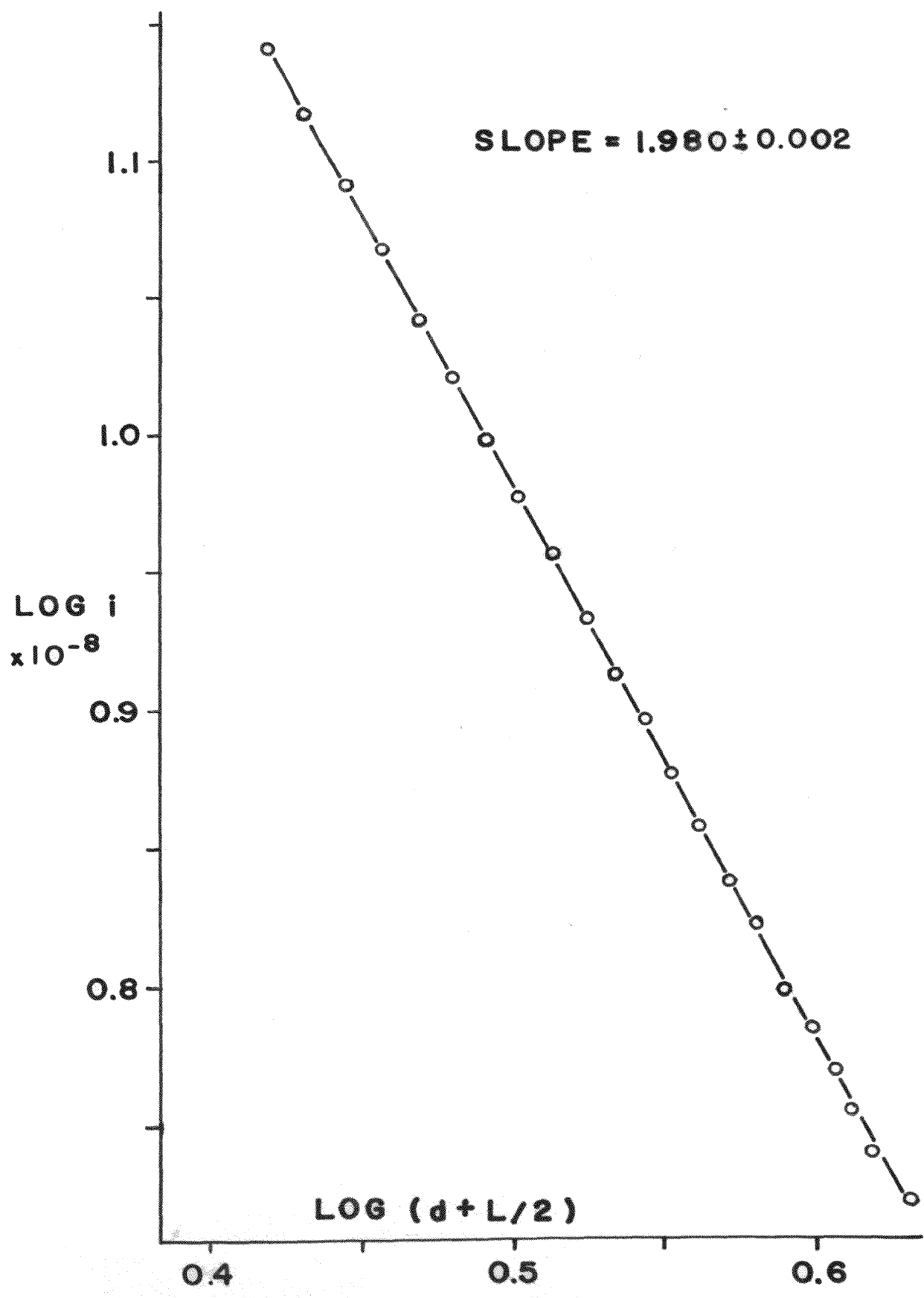


Figure 7

Table of Divergence Correction,
Alpha

Table for Finding Alpha at Various Plate Separations
With Window to Target Distance at 3.00 Inches

L	Alpha exponent=2.00	Alpha exponent=1.98
.020	1.0067	1.0067
.040	1.0134	1.0133
.060	1.0201	1.0199
.080	1.0268	1.0266
.100	1.0336	1.0333
.120	1.0404	1.0400
.140	1.0472	1.0468
.160	1.0540	1.0535
.180	1.0609	1.0603
.200	1.0678	1.0671
.220	1.0747	1.0740
.240	1.0816	1.0808
.260	1.0885	1.0877
.280	1.0955	1.0946
.300	1.1025	1.1015
.320	1.1095	1.1084
.340	1.1165	1.1154
.360	1.1236	1.1223
.380	1.1307	1.1293
.400	1.1378	1.1364
.420	1.1449	1.1434
.440	1.1520	1.1505
.460	1.1592	1.1575
.480	1.1664	1.1647
.500	1.1736	1.1718
.520	1.1808	1.1789
.540	1.1881	1.1861
.560	1.1954	1.1933
.580	1.2027	1.2005
.600	1.2100	1.2077
.620	1.2173	1.2150
.640	1.2247	1.2223
.660	1.2321	1.2296
.680	1.2395	1.2369
.700	1.2469	1.2442

equilibrium does not exist, then a systematic variation of the ratio with volume should be apparent. To correct for the inherent inhomogeneities due to the Aquadag film and the ion chamber window, the variable plate ionization chamber was used to obtain difference data on the specific ionization for a particular gas. This will give an energy deposition rate that is characteristic only of the ethylene gas. The limiting value of $\Delta\alpha_i/\Delta V$ as V increases without limit represents the specific ionization of the gas only, while the ratio of α_i/V includes the contributions of chamber inhomogeneities. Figures 8, 9, 10, 11 and 12 show the data used to correct for the chamber inhomogeneity for both the beryllium and the Aquadag window. Beryllium was chosen because it is frequently employed as the entrance window in analytical equipment for radiation chemistry studies using x-radiation. In using the beryllium window, a sheet of polyethylene of the same thickness as the aquadaged window was placed in the path of the x-rays. Likewise, with the aquadaged window, the beryllium was placed in the beam. This caused the x-rays to traverse the same medium before arriving at the inner surface of the front window. The beryllium window measured 0.0350 ± 0.0001 inches and the aquadaged polyethylene was cut from nominal two mil stock.

To eliminate inhomogeneity contributions in the data collected at a particular plate separation the correction

Figure 8

Integrated Specific Ionization Current
vs. Plate Separation for the Aquadag
Window, X-Ray: 70 kV @ 15 ma., 50 kV @
15 ma., 25 kV @ 20 ma., and 10 kV @ 20
ma., $d=3.00$ Inches; Plate Voltage =
10 kV/in.

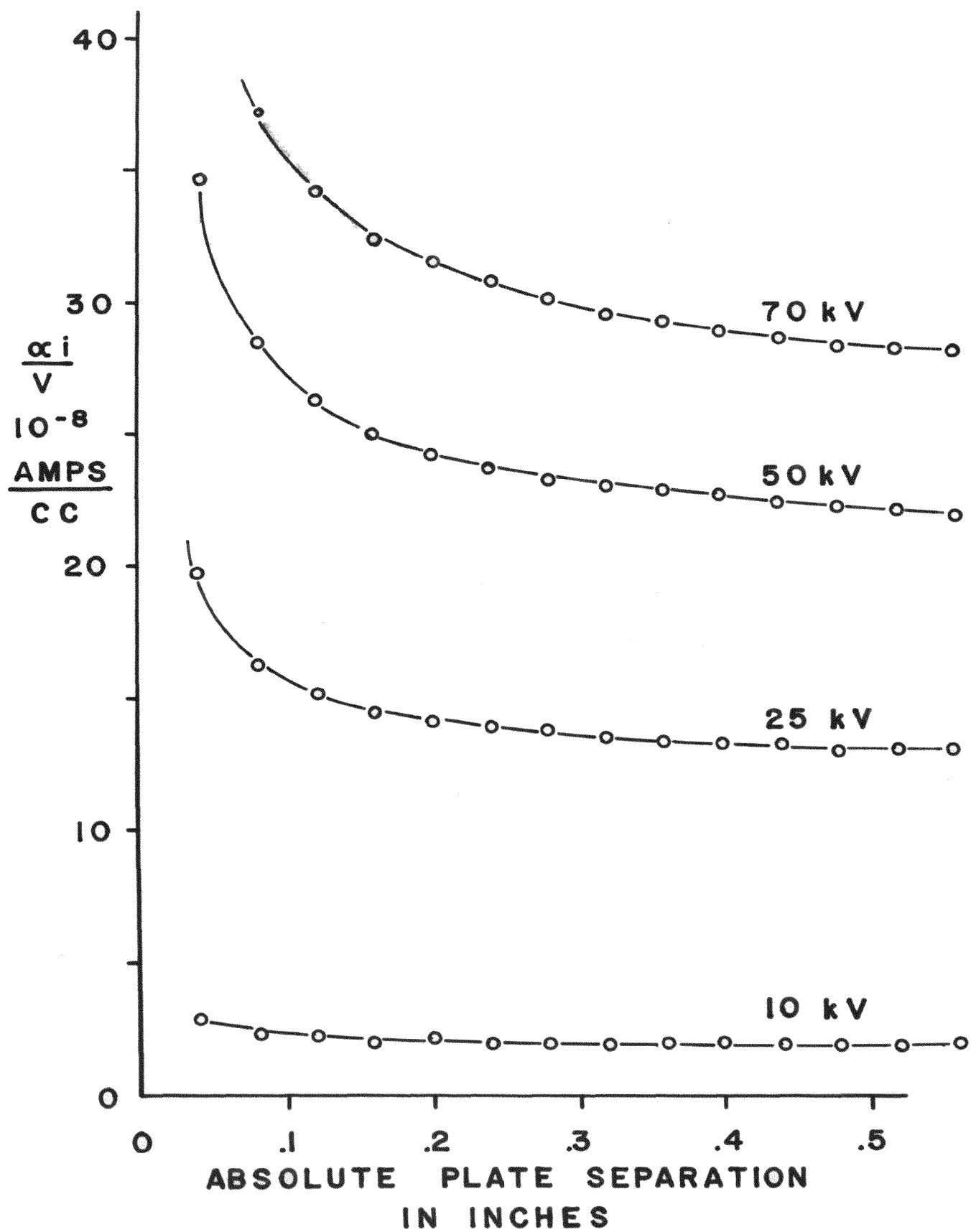


Figure 9

Differential Specific Ionization Current
vs. Plate Separation for the Aquadag Window
 $\Delta L=0.120$ inches, X-Ray: 70 kV @15 ma., 50 kV
@ 15 ma., 25 kV @ 20 ma., 10 kV @ 20 ma.,
 $d=3.00$ inches; Plate Voltage = 10 kV/in.

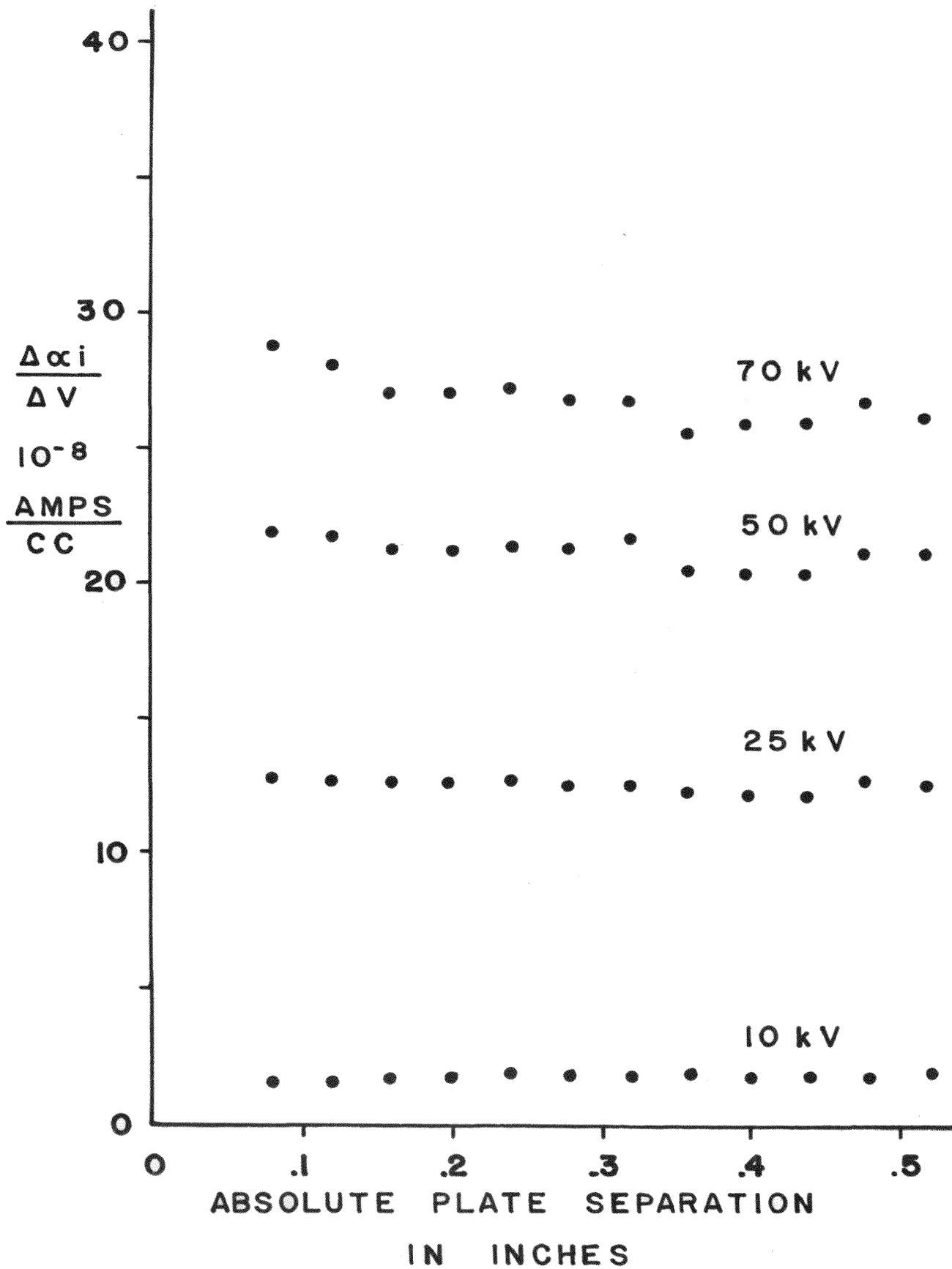


Figure 10

Integrated Specific Ionization Current
vs. Plate Separation for the Beryllium
Window, X-Ray: 70 kV @15 ma., 50 kV @
15 ma., 25 kV @ 20 ma., and 10 kV @ 20
ma., $d=3.00$ inches; Plate Voltage =
10 kV/in.

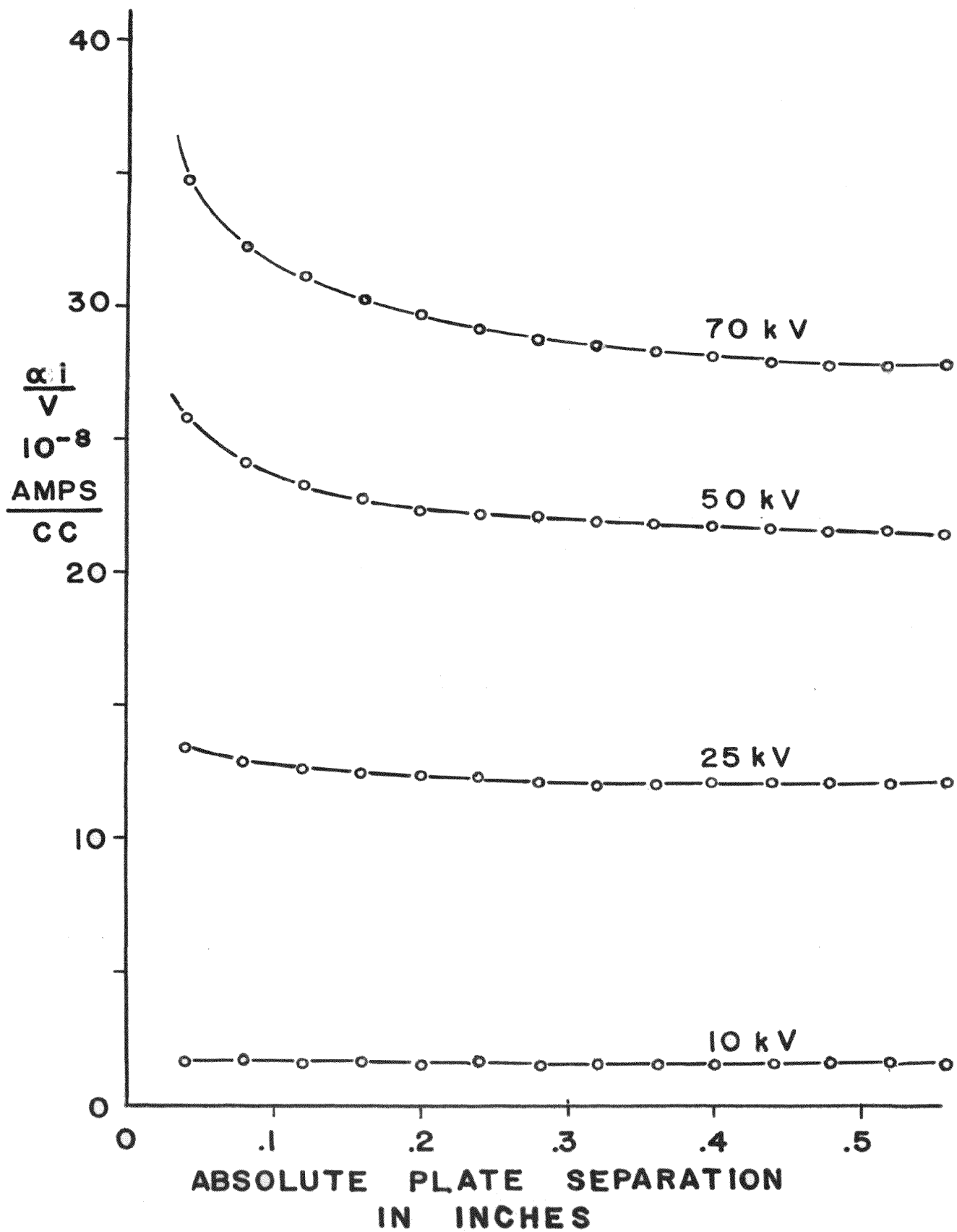


Figure 11

Differential Specific Ionization Current
vs. Plate Separation for the Beryllium
Window, $\Delta L=0.080$ inches, X-Ray: 70 kV @
15 ma., 50 kV @ 15 ma., 25 kV @ 20 ma.,
10 kV @ 20 ma., $d=3.00$ inches; Plate
Voltage = 10 kV/in.

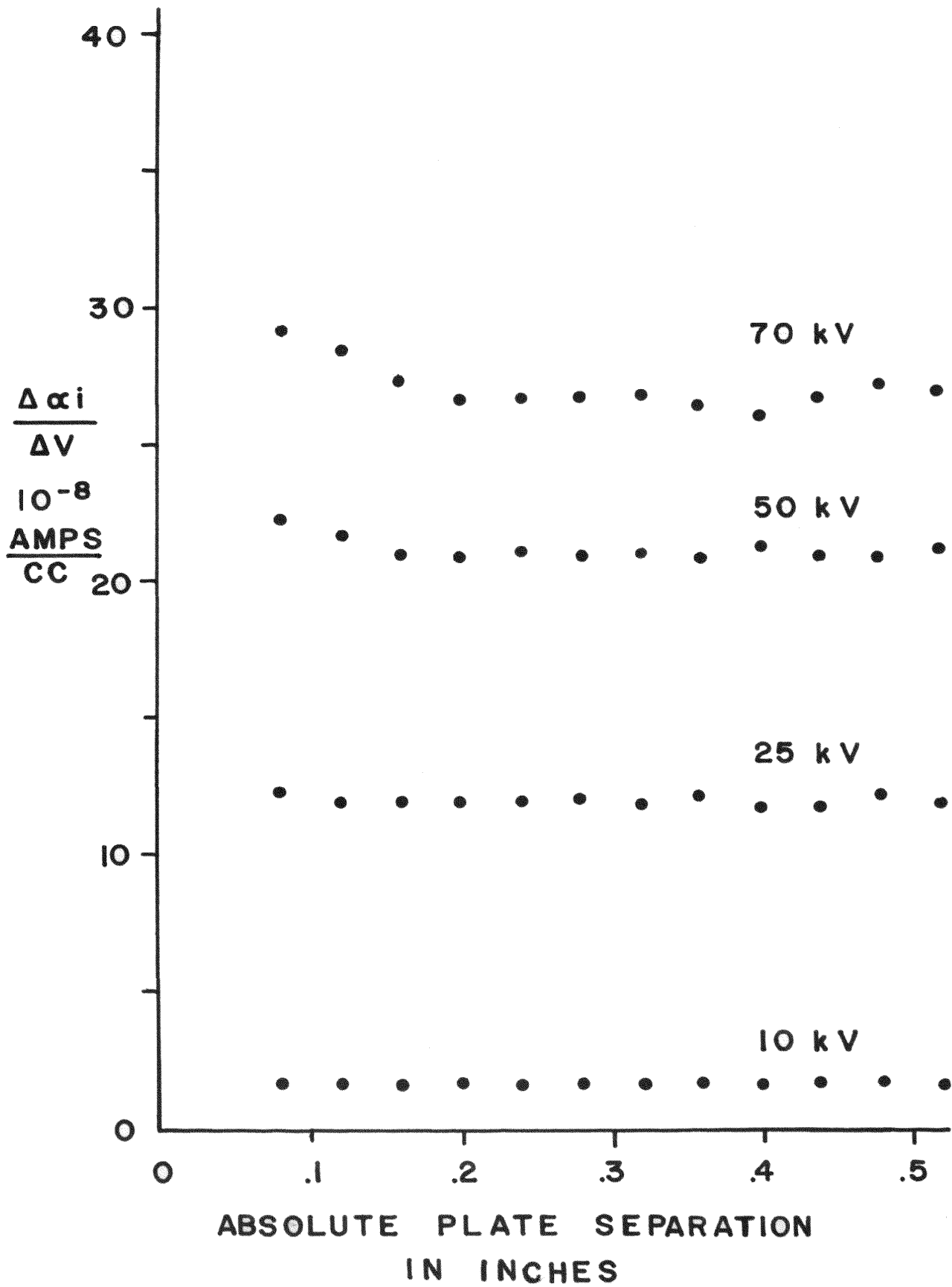
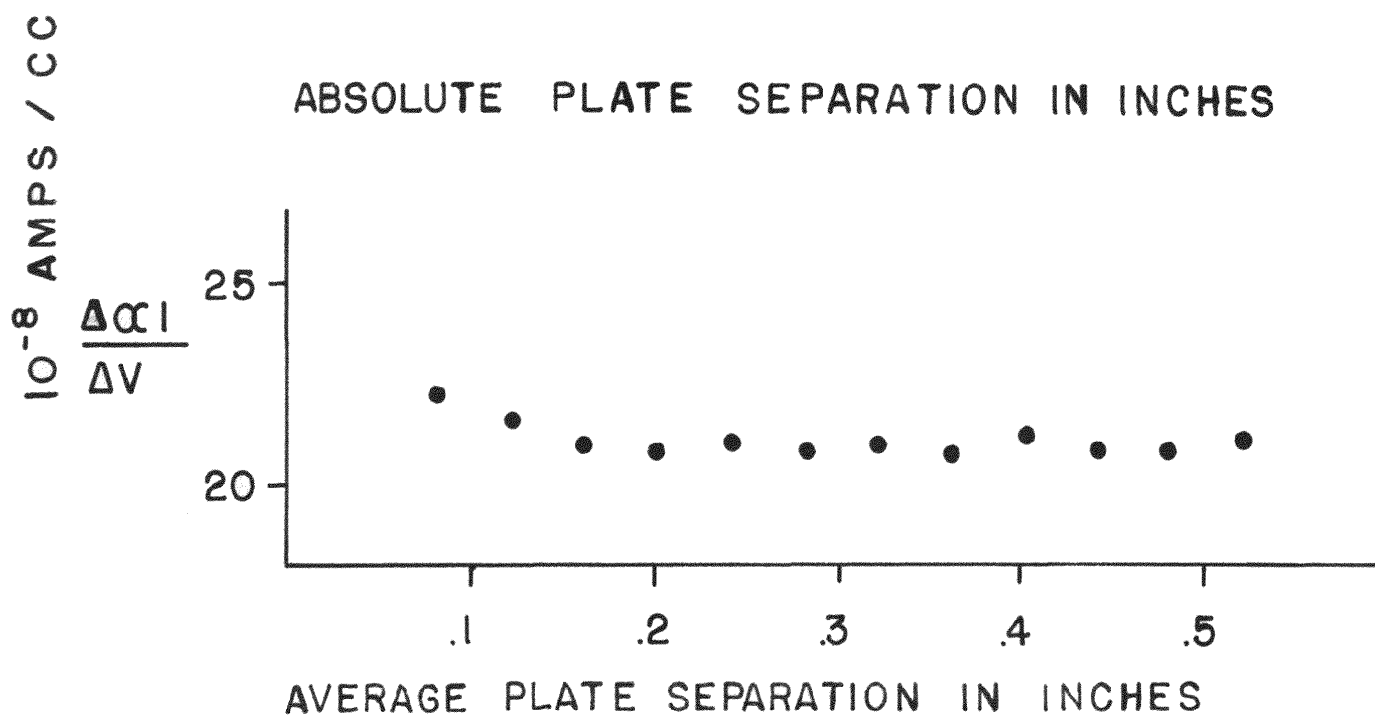
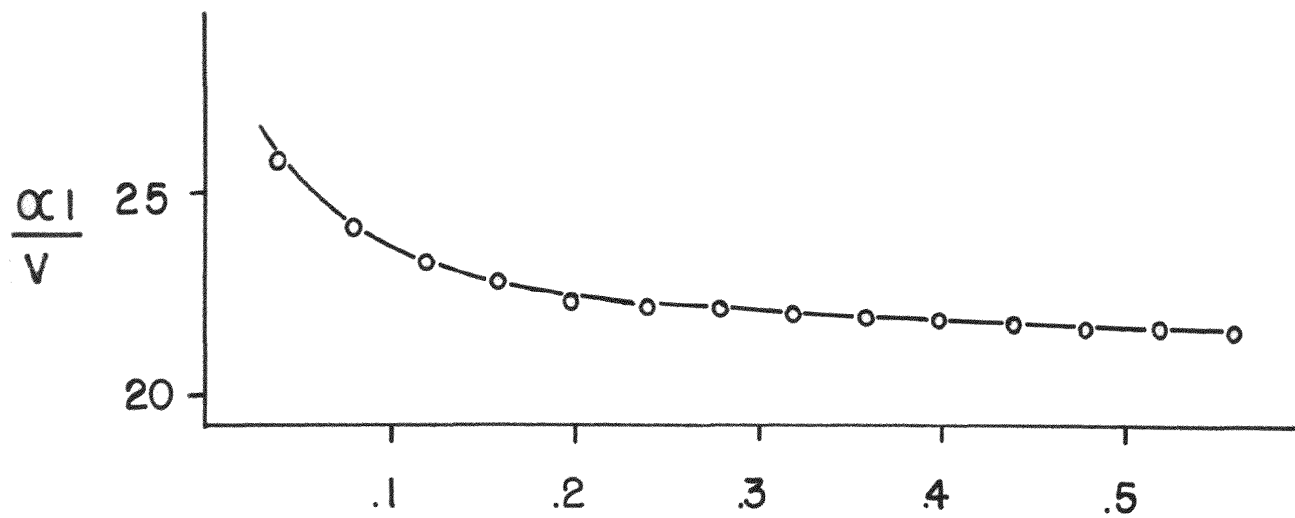


Figure 12

Comparison of Both Integrated and
Differential Specific Ionization
for Beryllium Window, X-Ray: 50 kV
@ 15 ma., d=3.00 inches; Plate
Voltage = 10 kV/in.



factor β defined by

$$\beta = \frac{\lim_{V \rightarrow \infty} \frac{\Delta \alpha_i}{\Delta V}}{\alpha_i/V} \quad (9)$$

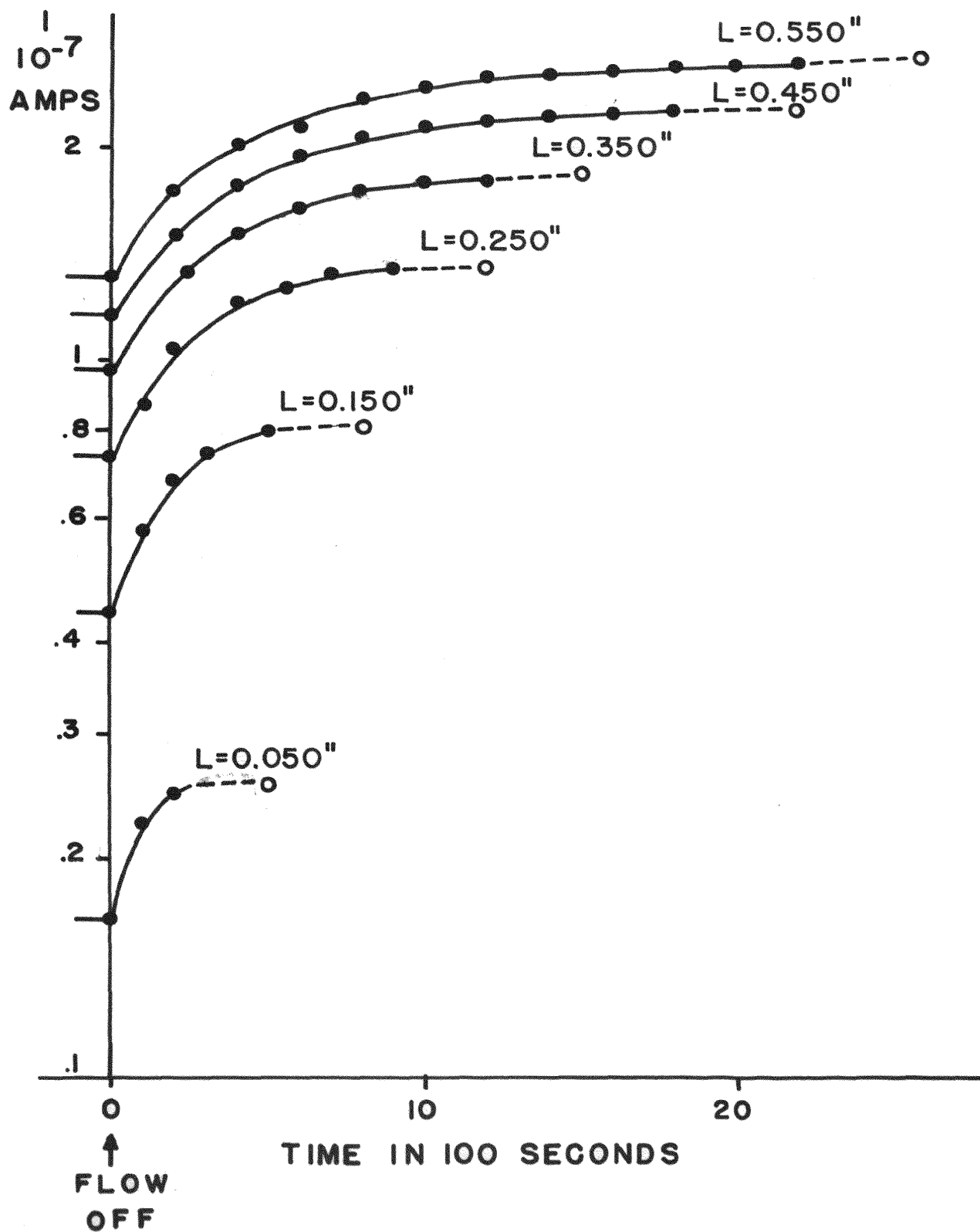
was applied. For example at a fixed plate separation of 0.300 inches β was found to be 0.96 ± 0.03 at 50 kV operation potential for the beryllium window. Figure 12 gives a good comparison of the integrated data and the difference data.

b. Flowing Gas vs. Static Gas

Since the radiation can be expected to alter the chemical composition of the cavity gas, the ion chamber was designed to continuously replenish the cavity gas. With a static system it can be seen that the ionization measured may not be entirely due to just the original cavity gas. The gas was flowed at a small, but sufficient rate to cause no change in ionization current when the flow rate was increased by a small amount. It was found that for the particular geometry used a flow rate of 180 cc/min. was necessary to meet the above criteria. Figure 13 illustrates the effect of an increase in ionization current with the use of a static system over that of a flowing system. The possibility of a temperature dependence of the cavity gas due to the presence of radiation was examined. After static equilibrium was reached, the x-ray source was turned off. It was then turned on

Figure 13

Ionization Current vs. Time After
Termination of Cavity Gas Flow, X-ray
was turned off at last ● and turned on
at o. X-ray: 70 kV @ 15 ma., Flow= 180
cm³/min., L=0.350 inches, d=3.00 inches



again after about an hour of time had passed and no change in ionization current was recorded. This indicated there was no temperature change in gas due to the presence of radiation.

c. Collection Efficiency

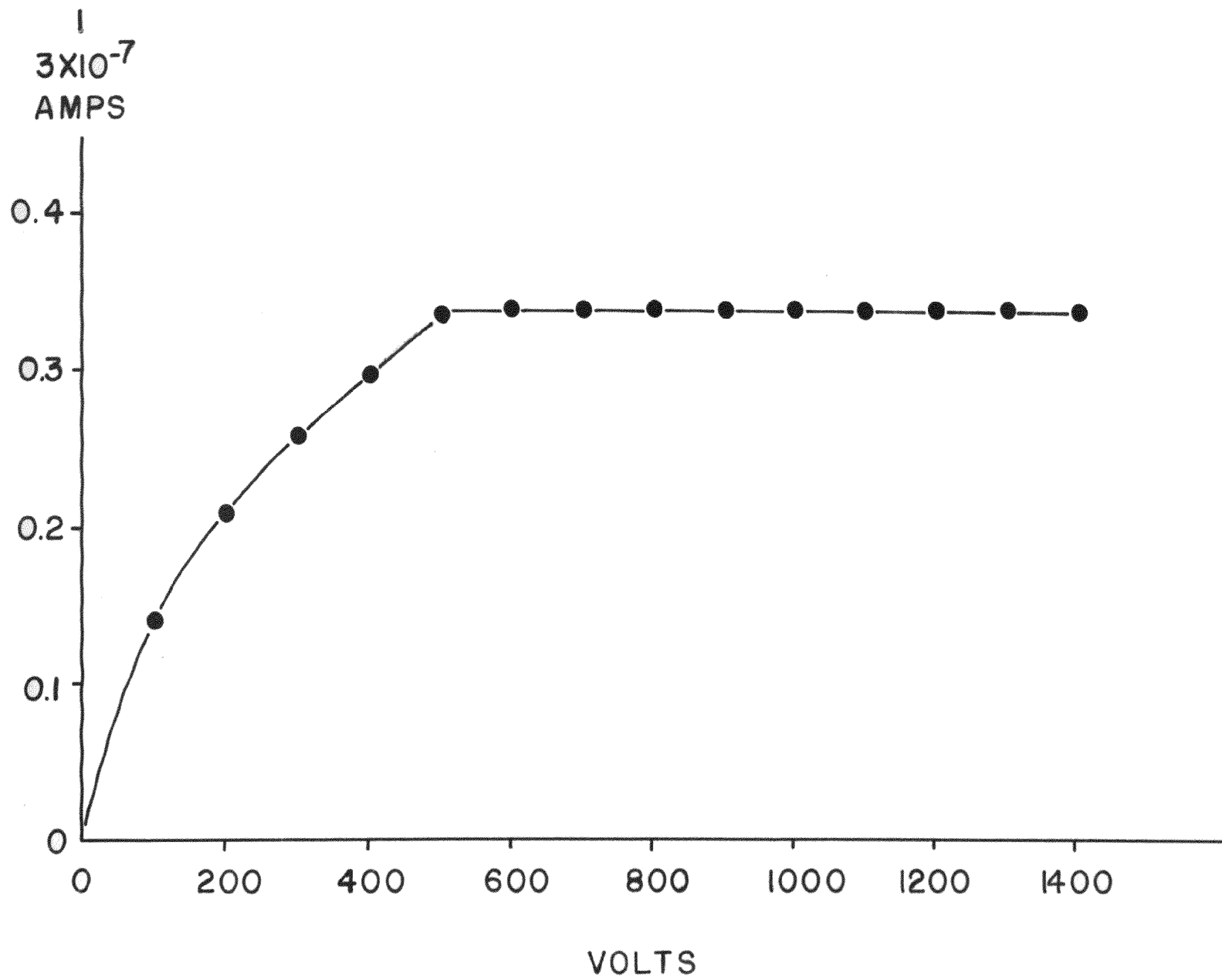
The expression for the collection efficiency was given in Chapter II. For a typical case, such as that of Figure 14, $d=0.350$ inches, $V=600$ volts, $i=1.0 \times 10^{-7}$ amps, and using $m=24.5$ (coulomb-sec) $^{\frac{1}{2}}$ cm. $^{-3/2}$, η is computed to be 1.2×10^{-12} , which corresponded to a collection efficiency of 100 percent. In order to be assured of a collection efficiency approaching 100 percent, the plate voltage was increased until a saturation of ionization current was observed. To maintain this high collection efficiency for various plate separations, the volume between the plates was maintained at an electric field considerably above that minimum which produces a saturation current for a given plate separation.

d. Dose Rate Profile as a Function of Depth

The rate of energy deposition in a material sample may be obtained by replicating the target-sample experimental geometry with the dosimeter replacing the sample. Layers of known thickness of sample material were then interposed between the ion chamber and the x-ray source

Figure 14

Plateau Voltage Characteristics for a
Plate Separation of 0.350 inches,
X-ray: 70 kV @ 15 ma., Flow=180 cm³/min.



and the resulting changes in the induced ionization current were monitored. In the present experimental study, layers of polyethylene were cut from two mil nominal stock with a circular cutter of two inches in diameter. Each layer was weighed and the respective mg/cm^2 was calculated. The ionization current measured for each successive layer of polyethylene generated a curve of dose rate as a function of sample thickness as shown in Figure 15. The target to chamber window distance was increased in amount corresponding to the thickness of the total number of layers, and the resulting ionization current was then measured. This corrects for the position of each successive layer of polyethylene with respect to the x-ray target. The average dose rate for a particular sample thickness may be computed by replacing the experimental curve with a rectangle having the same area, and reading the average dose rate from the value of the ordinate.

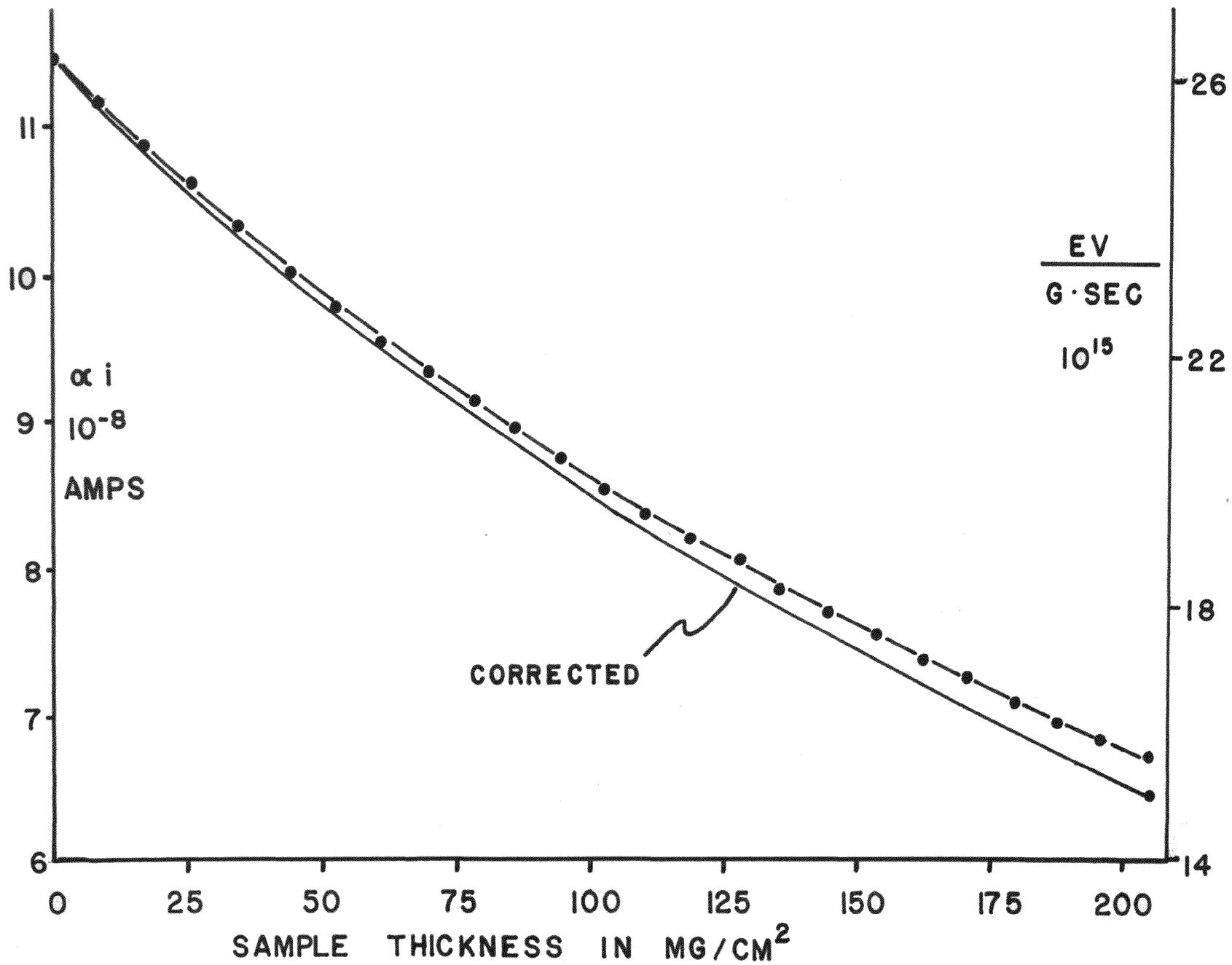
Operating at a plate separation L , the dosimeter essentially defines the dose rate at the back face of the sample for a sample equivalent thickness, t_s , defined by

$$t_s = \frac{\rho_0}{\rho_s} L \quad (10)$$

where ρ_0 is the density of the cavity gas and ρ_s is the density of the solid sample. For example, in these studies, $\rho_0 = 1.26 \times 10^{-3} \text{ gm cm}^{-3}$, $\rho_s = 0.96 \text{ gm cm}^{-3}$, and $L = 1 \text{ cm}$, gave a value of $t_s = 1.3 \times 10^{-3} \text{ cm}$.

Figure 15

Dose Rate vs. Depth
X-ray: 70 kV @ 15 ma.
d=3.00 inches, L=0.350
inches.



IV. RESULTS AND CONCLUSION

A. Differential Ionization

As Figure 12 shows, the differential ionization of the cavity gas with respect to the corresponding differential volumes ($\Delta\alpha_i/\Delta V$) is essentially in equilibrium at plate separations in excess of 0.100 inch. Hence, from a consideration of the density ratios of the gas to the solid, the electronic equilibrium can be expected from soft x-rays within the first few ten thousandths of an inch for similar solid materials. X-ray sources of this type, together with the dosimetry techniques described, provide an excellent method for radiation studies of thin samples.

Figure 12 shows the advantage of using the variable plate over the fixed plate separation ionization chamber. In spite of the fact that chamber inhomogeneities have been reduced by utilizing an extremely thin Aquadag film for the electrically conducting front window, it is evident that the integral method (α_i/V) may include a large contribution from secondary electrons arising from points other than the polyethylene body or the ethylene cavity gas. As can be seen, the error in using a fixed plate dosimeter is still significant even at large plate separations. The fixed plate data is extremely dependent upon the physical characteristics of the conducting film

on the front window. These effects are eliminated in the variable plate separation chamber.

B. Dose Rate Resolution

The maximum error in the dose rate can be deduced on the basis of experimental uncertainties in the measured quantities I and n. Assuming $F=F(x_i)$ and applying the calculus method of propagation of errors we have:

$$\frac{\Delta F}{F} = \left[\sum_i \left(\frac{\Delta x_i}{x_i} \right)^2 \right]^{1/2} \quad (11)$$

where x_i is the uncertainty associated with the quantity x_i .

$$\text{For } \frac{dD}{dt} = \frac{I W}{enM} = \frac{(\alpha\beta i)W}{e \left(\frac{PV}{\Omega_0 RT} \right) M} \quad (12)$$

we have

$$\frac{\Delta}{\frac{dD}{dt}} = \left[\left(\frac{\Delta\alpha}{\alpha} \right)^2 + \left(\frac{\Delta\beta}{\beta} \right)^2 + \left(\frac{\Delta i}{i} \right)^2 + \left(\frac{\Delta P}{P} \right)^2 + \left(\frac{\Delta V}{V} \right)^2 + \left(\frac{\Delta T}{T} \right)^2 + \left(\frac{\Delta W}{W} \right)^2 \right]^{1/2} \quad (13)$$

Assuming ΔW to be zero, equation (13) becomes:

$$\frac{\Delta}{\frac{dD}{dt}} = \left[\left(\frac{1.2 \times 10^{-3}}{1.120} \right)^2 + \left(\frac{0.03}{0.93} \right)^2 + \left(\frac{0.02}{1} \right)^2 + \left(\frac{0.45}{730} \right)^2 + \left(\frac{1.392 \times 10^{-3}}{6.31} \right)^2 + \left(\frac{0.1}{296} \right)^2 \right]^{1/2}$$

$$\frac{\Delta}{\frac{dD}{dt}} = [14.42 \times 10^{-4}]^{1/2} = 3.8 \times 10^{-2},$$

or 3.8 percent probable error in determining $\frac{dD}{dt}$, in addition to the unknown uncertainty in W . This error can be greatly reduced by improving the accuracy of the two largest contributions to the spread in resolution, namely β and i . The spread in β at 0.400 inches could have been due to an imperfection in the ion chamber at that point. However, upon investigation nothing out of the ordinary was found. Another source of the difficulties could be due to the suppression current in the picoammeter affecting the absolute scale. The picoammeter can be calibrated to a standard traceable to the National Bureau of Standards and hence, reduce the error associated with absolute current measurements to 0.25 percent. The value of W is common to every ionization method and hence does not affect the accuracy of the technique used in this experiment. As better values of W become available in the literature, dose rate data can always be renormalized to accommodate the increased precision. Furthermore, according to Whyte, W is independent of energy down to at least six kV and Ehrlich reports no incident spectral intensity below 10 kV. Therefore, the value of W should be invariant in these experiments.

APPENDIX

The Determination of Field Warpage

The method of investigation used to examine the electrical field in the dosimeter was to study two-dimensionally the electric field in a plane passing through the axis of the dosimeter. To do this a large model was constructed on Teledeltos Type L Paper* with the aid of conducting silver paint** for the electrodes.

Since Teledeltos paper is anisotropic, resistance measurements were made in both the transverse and lateral directions to determine the geometric correction factor to be employed in the model. The resistance varies directly as the length and as the inverse of the area for a normal conductor, hence, for a rectangle of T units wide and L units long, $R_T = C_1(T/L)$ and $R_L = C_2(L/T)$ where R_T and R_L are the resistances in the transverse and longitudinal directions respectively for the T by L rectangle. From the boundary conditions C_1 is the resistance in the transverse direction when $T=L$ and C_2 is the resistance in the longitudinal direction, also when $T=L$.

*Teledeltos Paper, an electrically conducting paper, is a product of Western Union Telegraph Co., New York, New York.

**General Cement No. 21-1

To obtain the geometrical correction factor R_L must equal R_T . Therefore, $C_1(T/L) = C_2(L/T)$, or $C_2/C_1 = (T/L)^2$. Hence, $T = (C_2/C_1)^{1/2}L$. C_2 and C_1 were measured to be $1886\Omega/\text{square}$ and $2105\Omega/\text{square}$ respectively. Therefore, $T = 0.946 L$. Thus, to correct for differences in resistances in the transverse and longitudinal directions, the model had a stretching factor of 1.056 in the longitudinal direction over that of the transverse direction.

The method of mounting the Teledeltos Paper that produced the most convenient arrangement for constructing the model was to affix the paper, aluminum coated side down, to a masonite board with rubber cement. All bubbles and wrinkles were then smoothed out.

Using a large model of the cross-section of the dosimeter, as mentioned earlier, a plot of equipotential lines was made using a regulated low voltage power supply applied across the electrodes and a precision D.C. voltmeter.

Approximating by eye, for the particular geometry used, a rule of thumb is that there is no warpage of the electric field bounded by the center one-third of the smaller disc.

BIBLIOGRAPHY

1. N.B.S. Handbook 85 (1964).
2. Aitken, J. H. and Dixon, W. R., N.R.C.(Can.), Report 4864 (1958).
3. Wang, P.K. S., Raridon, R. J., and Tidwell, M., Brit. J. Radiol., 30, 70(1957).
4. Ehrlich, M., Scintillation Spectrometry of Low Energy Bremsstrahlung, J. Res. N.B.S., 54, No. 2, 107(1955).
5. Epp, E. R. and Weiss, H., Phys. in Med. and Biol., 11, No. 2, 225(1966).
6. Whyte, G. N., Rad. Res., 18, 265(1963).
7. Ogier, W. T. and Ellis, D. V., J. Appl. Phys., 36, No. 12, 3788(1965).
8. Boag, J. W., and Wilson, T., Brit. J. Appl. Res., 3, 222(1952).
9. Erickson, Phil. Mag., 18, 328(1909).
10. Erickson, Phil. Mag., 23, 747(1912).
11. Boag, J. W., Phys. in Med. and Biol., 8, No. 4, 461(1963).
12. Nicholson, J. W., Phil. Trans. Roy. Soc., 224, 303(1924).
13. Love, E. R., Quart. J. Mech. & Appl. Math., 2, 428(1949).
14. Boag, J. W., Phys. in Med. and Biol., 9, No. 1, 25(1964).
15. Su, Gouq-Jen, Ind. Engr. Chem., 38, 803(1946).

VITA

H. Sajon Joyner was born 6 June, 1939, in Fort Worth, Texas, the son of Howard W. and Arista A. Joyner. Upon graduating from Arlington High School, Arlington, Texas, in June, 1957, he received a cooperative scholarship with Chance Vought, Inc., Dallas, Texas, and entered Arlington State College.

In September, 1960, he entered the University of Texas and was awarded the degree of Bachelor of Science in Physics in June, 1962 and a degree of Master of Arts in Physics in January, 1964. While at the University, he was employed as a Lecture Assistant in the Department of Physics for his first year and then as a Research Assistant in the Physics of Metastable Systems Laboratory sponsored by the Propulsion Sciences Division, Air Force Office of Scientific Research from June, 1961 to January, 1964.

From February, 1964 to July, 1964 he was employed by General Dynamics/Fort Worth as a Nuclear Engineer and then entered the Graduate School of the University of Missouri at Rolla in September, 1964. Upon entering, he became a Research Fellow at the Graduate Center for Materials Research of the Space Science Research Center of the University of Missouri.

Permanent address: 1611 West Second
Arlington, Texas

123745